25th ABCM International Congress of Mechanical Engineering
October 20-25, 2019, Uberlândia, MG, Brazil

COB-2019-1329
EXPERIMENTAL AND NON INVASIVE FUEL CONSUMPTION MEASUREMENT FOR INTERNAL COMBUSTION ENGINES BASED ON OTTO CYCLE

Emerson Alves da Silva
José Guilherme Coelho Baeta
PPGMEC – Programa de Pós-graduação de Mecânica da UFMG-Universidade Federal de Minas Gerais
Avenida Antônio Carlos, 6627, Pampulha – Belo Horizonte – MG – Brasil
emersonalves@cefetmg.br, baeta@demec.ufmg.br

Rodrigo Andrade Fonseca
CTM – Centro de Tecnologia da Mobilidade da UFMG-Universidade Federal de Minas Gerais
Avenida Antônio Carlos, 6627, Pampulha – Belo Horizonte – MG – Brasil
rodrigo-andradef@hotmail.com

André Guimarães Ferreira
DEMAT – Departamento de Engenharia de Materiais do CEFET-MG Centro Federal de Educação tecnológica de Minas Gerais
Av. Amazonas, 5253, Nova Suíça – Belo Horizonte – MG – Brasil
agferreira@cefetmg.br

Antônio Augusto Torres Maia
PPGMEC – Programa de Pós-graduação de Mecânica da UFMG-Universidade Federal de Minas Gerais
Avenida Antônio Carlos, 6627, Pampulha – Belo Horizonte – MG – Brasil
rodrigo-andradef@hotmail.com, aamaia@ufmg.br

Abstract. *This article describes a new methodology for measuring fuel consumption of internal combustion engines based on the Otto cycle and with Common Rail Injection System. The proposed technique requires only the measurement of the electrical signal pulses sent from the electronic injection system. The whole process does not demand any electrical, circuit breakage or direct contact with the fuel flow. The measuring system was built employing low-cost components, and its accuracy was evaluated using a Single Cylinder Research Engine (SCRE). It was performed a set of 32 tests, considering four different engine loads, four different speeds and two different fuels. The results obtained were superior to those achieved with electromechanical sensors, providing a fuel consumption measurement with a mean percent error inferior to 1.5% to Ethanol (E100) and inferior to 2.5% to blend of Gasoline end Ethanol (E27). As the methodology is based only on the electrical pulses, it can be considered applicable to an unlimited range of flow rate and pressure.*

Keywords: *fuel measurement, fuel consumption, Otto cycle, measurement of injection time.*

1. INTRODUCTION

When thinking about reducing fuel consumption and increasing energetic efficiency, it should be kept in mind that, in addition to a continuous improvement in the driver behavior (Wang and Rakha, 2016; Asad et al., 2011), it is also necessary to maintain a constant advance in the technologies and techniques for monitoring the fuel consumption in internal combustion engines.

To implement any control actions in fuel consumption, it is essential to know the fuel consumption at any instant of time, with a high degree of confidence (Asad et al., 2011). Meeting these requirements can be difficult, since the technologies available on the market today may present errors of about 10% (Furletec, 2013), making it impossible to obtain more accurate information on consumption. Despite all embedded technology present in automobiles nowadays, the cumulative fuel consumption is not available for most of the end users.

In most studies that assess the measurement of fuel consumption, it is suggested their techniques for doing so, such as: using Invasive Fuel Flow Sensors (Marcic, 1999); or evaluate the fuel quantity entering the injector, on the basis of the pressure-time variation occurring at one location along the rail-to-injector pipe, during the injection event (Ferrari e Paolicelli, 2017); or a specific software such as CUBE (Hakimelahi et al., 2016); or using some digital logic like *FPGA* (*Field Programmable Gate Array*) for injection time recognition (Pham, Vo, Jazar, 2017); artificial Neural Network (Du et al., 2017); simulations of the fuel consumption model (WT) in software like MatLab (Orfila et al., 2017).

The techniques based on electromechanical sensor installed in the fuel circuit of the vehicle require a complex and costly assembly and it violates the original system in which it will be installed what may result in a loss of credibility. Even the factory installed on-board computers present in many vehicles are not suitable, a priori, for measuring the accumulated fuel consumption, because this feature is out of its main purpose and these systems can be reset at any time by any individual, thus rendering it useless as a fraud-proof measuring instrument.

In the current literature, several authors stressed the importance of having a real-time measurement of fuel consumption; some suggest attractive ideas, such as (Herdzik, 2016) that reinforces the idea of measuring the fuel flow in the camera for that there is a control of the harmful emissions gases. In their work the information on the flow is given by the survey of the characteristics of the Injector Nozzle, Injection Pump and the fuels that operate by them, and to measure them, the author points to Kinetic Viscosity of fuels as one of the main factors that influence in the flow rate thereof, together with the flow velocity and the turbulent or laminar behavior assumed by the fuel as it passes through the orifice of the nozzle. In this way, the author defines a flow coefficient related to the fuel flow that passes through the nozzle, and that will be used in the calculations; in work carried out by (Espinosa et al., 2011), the importance of monitoring fuel consumption for the mitigation of harmful combustion gases is again emphasized. In order to achieve this monitoring, the author proposes the construction of equipment to monitor some conditions and parameters of the vehicle in situations of use in real traffic, using information from OBDII and other autonomous sensors. Such equipment measures the variation of mass of fuel or the redundancy of information provided by the OBDII system, and thus obtains the consumption in g/s (gallons per second).

In work proposed by (Farooqi, Snyder, and Anwar, 2013) it was proposed to use Field Programmable Gate Array (FPGA) and DMA (a type of Randon Access Memory) to store and interpret the injection pulses and optimize the algorithm to find the best start and end thresholds of the periods of injection. Once the injecting periods had been captured and identified, what he calls the "on time" of the injectors, the information was registered and accumulated.

This work aims to develop an embedded system to measure and accumulate the fuel consumption of an internal combustion engine, based on the Otto cycle and with Common Rail Injection System. The proposed system is intended to be easily accessible and low cost. It is believed that its use can contribute for studies of fuel consumption, control optimization, maximization of the performance of engines in different driving scenarios, and training of drivers as to their form of driving, thus enabling the so-called eco-driving (Orfila et al., 2017).

2. MATERIALS AND METHODS

2.1 Experimental setup

The tests were carried out in the Single Cylinder Research Engine (SCRE) and the platform of acquisition and monitoring of the test bench consists of four different systems: PUMA (monitors the dynamometer data), INDICOM (Responsible for the acquisition and monitoring of pressure inside the cylinder and in the intake and exhaust manifolds.), NAPRO (measures the amnesia of the four major gaseous pollutants, CO, CO2, NOx and HC), ETU (makes electronic engine management).

Through this platform it is possible to monitor the following physical quantities: engine fluid temperature, air flow, fuel flow, lambda, temperature and pressure in the regions of interest, and it is also possible to calculate the specific consumption and fuel conversion efficiency, pressure acquisition and monitoring inside the cylinder, the ignition timing, the fuel injection, the injection time and the direct injection line pressure. Table 1 shows the technical features of some instruments used to the tests.

Table 1 - Technical characteristics of instrumentation.

Parameter	Manufacturer / Model	Type	Measuring Range	Origin of Uncertainty	Uncertainty (Type B)
Rotation speed	AVL 365	Optical	50 a 20000 rpm	Manufacturer	< ±0,03%
Pressure in the combustion chamber	AVL GU22CK	Piezoelectric	0 a 350 bar	Manufacturer	±0,3%
Pressure at admission	AVL LP11DA	Piezoelectric	0 a 10 bar	Manufacturer	±0,1%
Balance of fuel	AVL 733S	Gravimetric	0 a 160 kg/h	Manufacturer	±0,05%
Fuel temperature	PT100	Resistive	-50 a 650 ºC	Calibrated	±0,7%

According to (ANP, 2017), the specific mass is non-standardized to blend gasoline with ethanol 27% ±1, however, according to (Sindi Petróleo, 2015) its specific mass ρ is normally between 734.0 and 743.0 kg/m^3, so in this work the mean value of 738.5 kg/m^3 will be appreciated for gasoline (E27) to 25 degrees Celsius.

Still according to (Sindi Petróleo, 2015) the pure ethanol (E100) has a specific mass normally between 799.81 and 810.85 kg/m^3, so in this work the mean value of 805.33 kg/m^3 will be appreciated for ethanol (E100) to 25 degrees Celsius.

The value of 25 degrees Celsius was chosen because it is the set point temperature for our fuel for the tests performed in the SCRE.

2.2 Measuring system

An embedded system was built using a PIC18F452 I/P microcontroller with a capture circuit capable of measuring duration time of an electric pulse with a resolution of 3.2us. With this system it was possible to measure each injection pulse sent to the electric fuel injector, comparing the accumulated fuel mass at the end of each test, as well as the values of rpm, mass flow, and volumetric flow, performed in all scenarios.

In each experiment, a different rpm speed and the axle load were used according to the intake pressure. Thus, the velocities of 1000, 2000, 3000 and 4000 rpm were used, and 400, 600, 800 and 921mbar were used for the inlet pressures, the last pressure is equivalent to the local atmospheric pressure, with the throttle valve fully open. All these tests scenarios were performed using pure Ethanol (E100) and using Gasoline with 27% of Ethanol (E27). Each test lasted 90 seconds.

As the methodology proposed in this work was based only on the analysis of the injection duration time, it was not used any other data from the motor operation.

The fuel that enters in the duct that leads to the explosion chamber has a controlled temperature that is not changing more than 0.2°C because this parameter is one among others controlleds by university laboratory. The mean volumetric expansion coefficient for pure gasoline is $1.2 \times 10^{-3}\ ºC^{-1}$, which did not entail a significant error in the measurements. That is why the fuel temperature is a parameter that was considered constant in the calculations. This hypothesis dispensed the installation of a second temperature sensor for the fuel. Thus, in this work, the fuel was considered as an incompressible fluid, which means that the parameter ρ remains constant.

Most injection systems currently work with a pressure regulator at the Common Rail. To better understand the influence of this pressure, some research works have been made. The study presented by (Szpica, 2018) pointed out that the pressure variations at the entrance of the combustion chamber can influence the fuel consumption measurements. However, the final error remained between 0.5% and 3%. In the article by (Farooqi, Snyder, and Anwar, 2013), which also attempts to observe the influence of fuel inlet pressure, the authors consider that the pressure variation was insignificant. Based on these studies, in this work, the pressure at the inlet of the injector was considered constant.

Figure 1 (a) shows the general electrical schematic, (b) shows more details about the Current Probe installed on fuel injector cable, (c) shows more details about the mono cylinder of the laboratory.

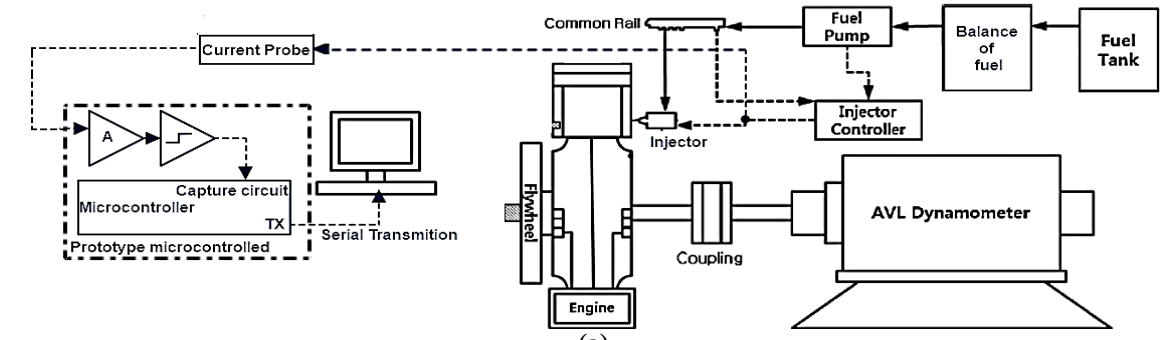

(a)

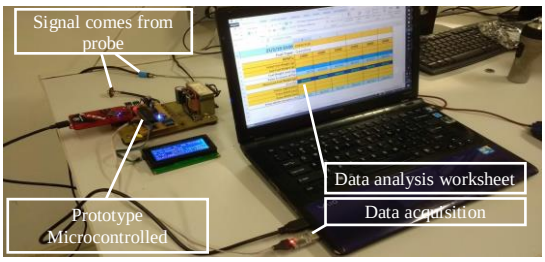

(b)

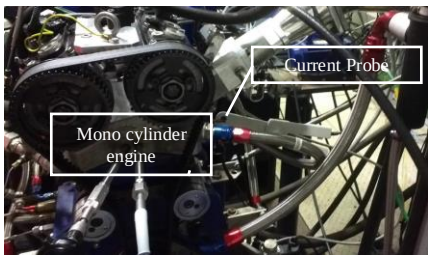

(c)

Figure 1 – (a) SCRE control bench, (b) Current Probe installed on fuel injector cable, (c) Hardware for the measures

The injection pulses were measured through a current probe, so the fuel injector drive current could be detected. The output signal of the current probe first was conditioned by an operational amplifiers stage to turn it compatible with the digital`s level of the controller stage, and so, allow identifier the “opening time” and “closing time” of the injection pulses. Figure 2 (a) shows the Current Probe (Keysight Technologies, 2019). Figure 2 (b) and (c) respectively show details of the input signal from the Current Probe and the signal already processed to be recognized by the digital circuit.

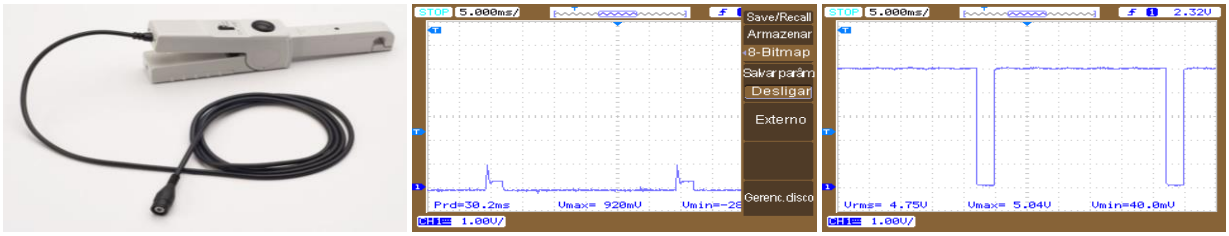

(a) (b) (c)

Figure 2 – Characteristics of the input signal; (a) Current Probe model 1146b Keystone (Keysight Technologies, 2019) ; (b) Electronic signal detected by Current Probe; (c) Treated digital signal to digital TTL voltage levels.

The duration of each identified event was measured by a microcontroller with a specific hardware circuit with a timing function. The resolution of this process was of 3.2us, which is more than 300 times smaller than the normal injection pulses in a vehicle.

The electronic schematic of the prototype can be seen in fig 3. For the design of the prototype, there was the concern of maintaining a low-cost electronics and easy access in electronic components markets. The microcontroller chosen was PIC18F452, for which the datasheet can be accessed in (Tecnology Inc., 16 Feb 2019).

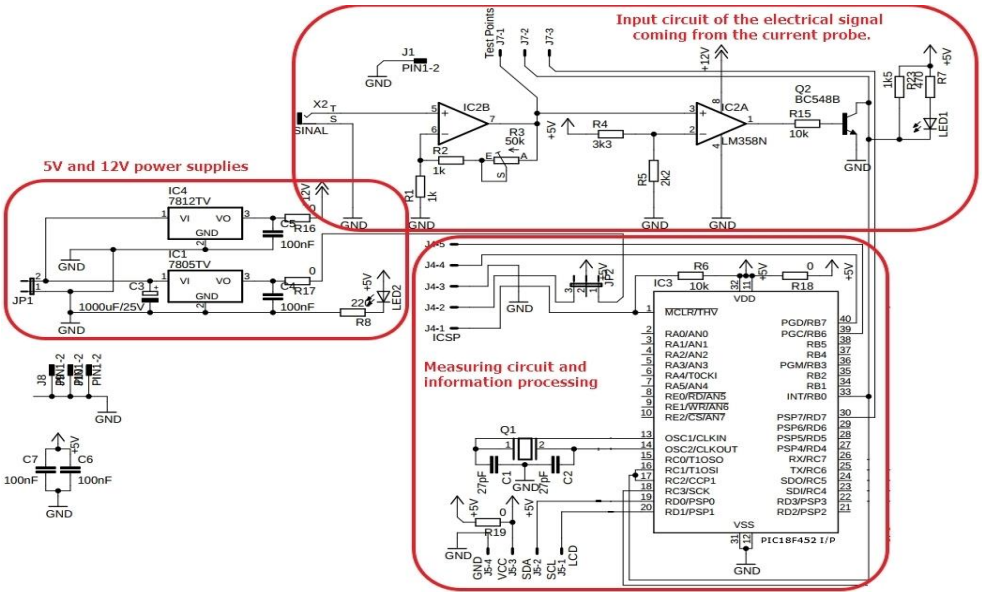

Figure 3 - Electronic Prototype Scheme for validation of the Methodology.

All injection pulses were exported in a text-type file and for each one, the prototype generated a new line within the logging file containing the pulse duration, in milliseconds, the sequential number of that pulse within the test time, and, finally, the time in which this pulse has occurred since the beginning of the test, also in milliseconds. Subsequently, the data of all the injection pulses were imported into a spreadsheet where they could be analyzed. Thus, important information about each test could be removed such as the rpm speed at which the engine was located, the average size of the injected pulses, and the total time of fuel injection. Figure 4 shows a portion of a text file after it has been imported into the spreadsheet.

time [s]	Pulse Number	Pulse Width [ms]
0.016	1	1.72480
0.056	2	1.72480
0.096	3	1.72480
0.136	4	1.72480
0.176	5	1.73120
.	.	.
.	.	.
.	.	.
89.816	2246	1.71840
89.856	2247	1.72160
89.896	2248	1.72160
89.936	2249	1.72160
89.976	2250	1.71840
	Total injection time[ms]:	3826.4672

Figure 4 - Data on all injection pulses performed in a 90 second test and imported into the spreadsheet.

The summary of the measured results by the prototype was compared with the official results obtained during the experimental tests.

2.3 Mathematical formulation

For the fuel flow that crosses the body of the fuel injector, until reaching its outlet to the explosion chamber, the Bernoulli equation can be applied to the flow through the reduction of area, considering it ideal and taking reference lines between points 1 and 2, according to fig. 5.

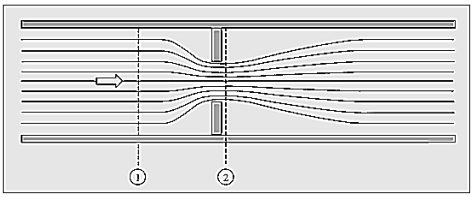

Figure 5 - Flow with Throat

The Bernoulli equation without loss of load applied to the ideal flow between points 1 and 2 of fig. 5 gives Eq. (1):

$$\frac{{U_1}^2}{2} + \frac{P_1}{\rho} + gz_1 = \frac{{U_2}^2}{2} + \frac{P_2}{\rho} + gz_2 \tag{1}$$

In which U_1 and U_2 are respectively the fuel speeds at the inlet (common rail) and outlet (blast chamber) of the injector. P_1 and P_2 are respectively, the pressures inside the injector and the chamber. Z_1 and Z_2 are respectively the sea level heights for the fuel particle within the injector and the chamber, which in this case can be considered equal due to their proximity.

According (Figliola, Richard S., 2011) there are three common types of flow meters: per orifice plate; the venturi; and the flow nozzle. Among these types, it can be seen that the fuel injector characterizes a situation of the type Square-edged orifice plate. Using the mass conservation equation between sections 1 and 2 for incompressible flow gives:

$$\overline{U}_1 = \overline{U}_2 \frac{A_2}{A_1} \tag{2}$$

In which A_1 and A_2 are respectively the areas at the inlet and outlet of the injector. Then substituting Equation (2) into Equation (1) and rearranging yields the incompressible volume flow rate can be obtained by:

$$Q_I = \overline{U}_2 A_2 = \frac{A_2}{\sqrt{1-(A_2/A_1)^2}} \sqrt{\frac{2(P_1 - P_2)}{\rho}} \tag{3}$$

In witch the subscript *I* emphasizes that Eq. (3) gives an incompressible flow rate.

When the flow area changes abruptly, the effective flow area immediately downstream of the area reduction is not necessarily the same as the pipe flow area (Figliola, Richard S., 2011). When fluid cannot exactly follow a sudden expansion of area due to its inertia, a central core flow called the vena contracta forms that is bounded by regions of slower flow, with vortex recirculation. As a consequence, the pressure measured with the wall taps of the pipe will correspond to the highest flow velocity within the vena contracta with its unknown flow area, A_2. To account for this unknown, it is introduced a contraction coefficient C_C, where $C_C = A_2/A_0$, with A_0 based on the meter throat diameter, into Eq. (3). This gives

$$Q_I = \frac{C_C A_2}{\sqrt{1-(C_C A_2/A_1)^2}} \sqrt{\frac{2(P_1 - P_2)}{\rho}} \tag{4}$$

Furthermore, according to (Figliola, Richard S., 2011) , other effects such as frictional head losses can be incorporated into a friction coefficient, C_f, such that Eq.4 becomes

$$Q_I = \frac{C_f C_C A_2}{\sqrt{1-(C_C A_2/A_1)^2}} \sqrt{\frac{2(P_1 - P_2)}{\rho}} \tag{5}$$

For convenience, the coefficients are factored out of Eq. 5 and replaced by a single coefficient known as the *discharge coefficient (C)*, which, in the end, represents the ratio of the actual flow to the ideal possible flow rate for the fall of the measured pressure. Reworking Eq.(5) leads to the incompressible operating equation

$$Q_I = \rho^{-0.5} \frac{CA_0}{\sqrt{1-(A_0/A_1)^2}} \sqrt{2\Delta P} \tag{6}$$

The flow behaviors of the orifice plate have been studied to such an extent that these meters are used extensively without calibration. Values for the discharge coefficients, flow coefficients, and expansion factors are tabulated and available in standard U.S. and international flow handbooks along with standardized construction, installation, and operation techniques. Because each fuel injector has its specific design, and because it does not have tabulated values, Eq. (6) must be adjusted by a parameter with a value to be found through the calibration process, as indicated by (Figliola, Richard S., 2011).

As the methodology presented in this paper proposes the measurement of the total mass of fuel, and knowing that this mass is given by

$$m_{total} = \dot{m}.\Delta t_i \tag{7}$$

In which the total mass, m_{total}, of fuel consumed is obtained by multiplying the mass flow rate, $\dot{m}$, by the total injection times in seconds (Δt_i), or rather, the sum of all durations of the electric pulses of injection sent from the electronic controller unit of the vehicle to the electro-injector, and it was accurately measured by the capture circuit present in the measuring system proposed. In the same way, the mass flow rate can be obtained by multiplying the volumetric flow rate by the specific mass (ρ) of the fuel used. From Eq. (6) it can be seen that, all parameters are constant and are related to the physical quantities of the injection system in question, and for convenience will be represented by a unique coefficient called Calibration Coefficient, $C_{calibration}$, and the coefficient ρ is related to the fuel used. Thus, working Eq. 6 with Eq. 7 gives

$$m_{total} = \Delta t_i.\sqrt{\rho}.C_{calibration} \tag{8}$$

Where the $C_{calibration}$ must be found through a calibration process for each different injection system, in other words, for each type of injection system for which the methodology is to be implemented. Over time, a database with $C_{calibration}$ values can be implemented for all makes and models of vehicles on the market, and after that information, also the type of fuel to be used and then the equipment to be implemented the methodology will be able to report the amounts of fuel mass consumed in real time.

As the tests of this work were carried out in controlled environment, it was possible to verify by the generated worksheets indicated an effective thermal amplitude in the fuel inferior to 1° Celsius. This thermal amplitude less than 1° Celsius for gasoline, which has volumetric expansion coefficient in the order of $1.2x10^{-3}x^{o}C^{-1}$, represents an error in the order of ±0.12% error in the measurements. Therefore, the temperature of the fuel is a variable that will be considered constant in our calculations. This simplifying assumption will make dispensing the installation of a temperature sensor for fuel for the implementation of the methodology unnecessary. Thus, from this point the fuel will be considered as an incompressible fluid, which means that the parameter ρ (kg/m^3) will remain constant for the measurements to be performed.

The surveys of (Szpica, 2018) pointed out that the pressure variations at the entrance to the explosion chamber can affect the mass flow measurement error, the final error variation remained in the order of 0.5% to 3% using gasoline as fuel. In the paper by (Farooqi, Snyder, and Anwar, 2013), which also tries to observe the influence of the fuel inlet pressure, the authors consider in their experiment that the pressure variation in the Rail is insignificant. In view of this, it can be seen that, from the point of view of the variation in the inlet pressure of the chamber, which is in the range of 400 to 921 mbar, it represents less than 1% of the pressure inside the rail, which is in the range of 100 to 120 bar, thus, the methodology proposes as a simplifying hypothesis, to consider the constant pressure delta.

According to (Heywood, 2018), the nozzle or electro-injector is an electronically controlled fuel injection valve which, when not energized or energized, its solenoid ceases its magnetic field allowing the return spring to force the plunger to close where it would pass the fuel to the chamber, blocking the fuel. Whereas, when receiving an electrical excitation signal, the electro-jet solenoid coils the magnetic field that overcomes the return spring force and opens the piston allowing the fuel flow into the chamber for the time pre-established by the map injection in the vehicle's ECU.

According to (Herdzik, 2016), the amount of injected fuel into the cylinder with electromagnetic injector depends mainly on the injector opening duration. Thus, proceeding with the implementation of the methodology, the project is initiated for an electronic prototype that will implement the measurements of all the electronic injection pulses that enable the fuel flows inside the vehicle's explosion chamber. With the prototype, fuel consumption tests were performed using three different fuels: pure ethanol (E100), petrol mixed with 27% ethanol (E27), and pure gasoline (E0). With each type of fuel, 16 different scenarios composed of four different speeds and four axle load values.

At the end of each test, two important pieces of information that are the basis for the next analyzes are the total mass of fuel consumed in the test, reported by the laboratory scale, and the total sum of the injection times of each pulse sent to the electro-injector, measured by the prototype. The final mass of fuel consumed divided by the total injection time, will define the calibration factor of the equipment. This parameter, given in grams per second, will allow the prototype to estimate the correct mass of fuel consumed only with the measurement of the injection pulses.

After calculating the ratio in grams per second in each test, the value was used in the conversion of all injection times of each particular pulse in mass of fuel. Next, the final mass value indicated by the prototype was compared with the final value of mass consumed indicated by the scale, and the errors could be calculated with the Eq. 9:

$$Error_{percent} = \left(\frac{m_{total_{measured}} - m_{total_{theoric}}}{m_{total_{theoric}}} \right) . 100\% \tag{9}$$

Equation 9 provids the percent error that represents an information when working directly with the consumption control, since it indicates how significant is the deviation between the actual consumption and the consumption measured by the methodology.

3. RESULTS

The percentage errors of all tests varied from 0.16% to 8.74%, and indicates an average value of 3.18% for Gasoline (E27) tests, and from 0.10% to 3.30% and indicates an avarege value of 1.51% for Ethanol (E100) tests. These values represent the best possible average error for the system as a whole, that is, it incorporates all physical factors such as flow, pressure, temperature, fluid properties and errors of the equipment involved, so it is expected that the methodology applied to any tests performed on this engine with these fuels present at least these calculated average errors.

Looking at the graphs in fig. 5, it can be seen that all the results have very close values because of the low percentage error. This was already expected since each scenario illustrated in Fig. 5 was generated from a calibration parameter calculated for this specific test and after the same. For the situations where the actual amount of fuel to be consumed and measured is not known beforehand, the prototype was already programed with a fixed and optimized value of the calibration parameter. This parameter was optimized based on the calibration test information already performed. Therefore, from the calibration values found in the above calculations, a weighted average was calculated, and the result was used as a fixed calibration value, and also the fuel mass values provided by the prototype were recalculated based on this new optimized value of calibration.

The Fig. 6 (a) to (d) show the best possible results for particular tests were expressed in graphs first to have visual proof of the validity of the test and an estimate of its accuracy.

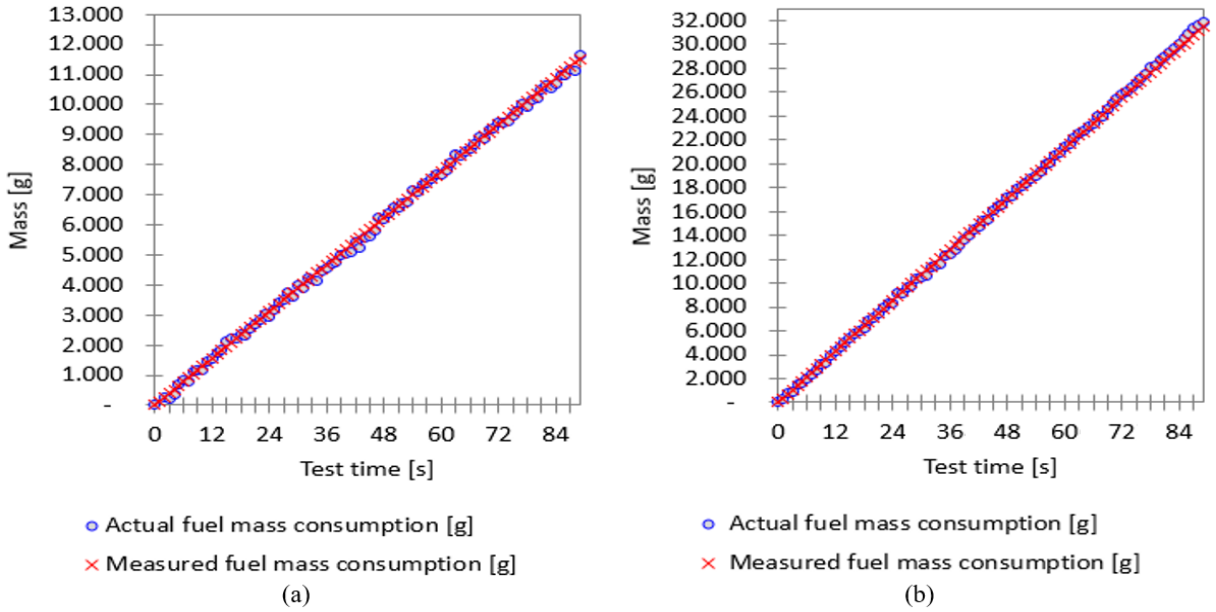

Figure 5 – (a) and (b) shows ethanol mass consumption tests with 1000rpm and inlet pressures equal to 400 and 921mbar, respectively. Each graphic was generated using its specific calibration value.

The fig. 6 (a) and (b) show the first two graphs of a series of 16 in all, recalculated based on the new value of the fixed calibration parameter and already previously recorded in the prototype.

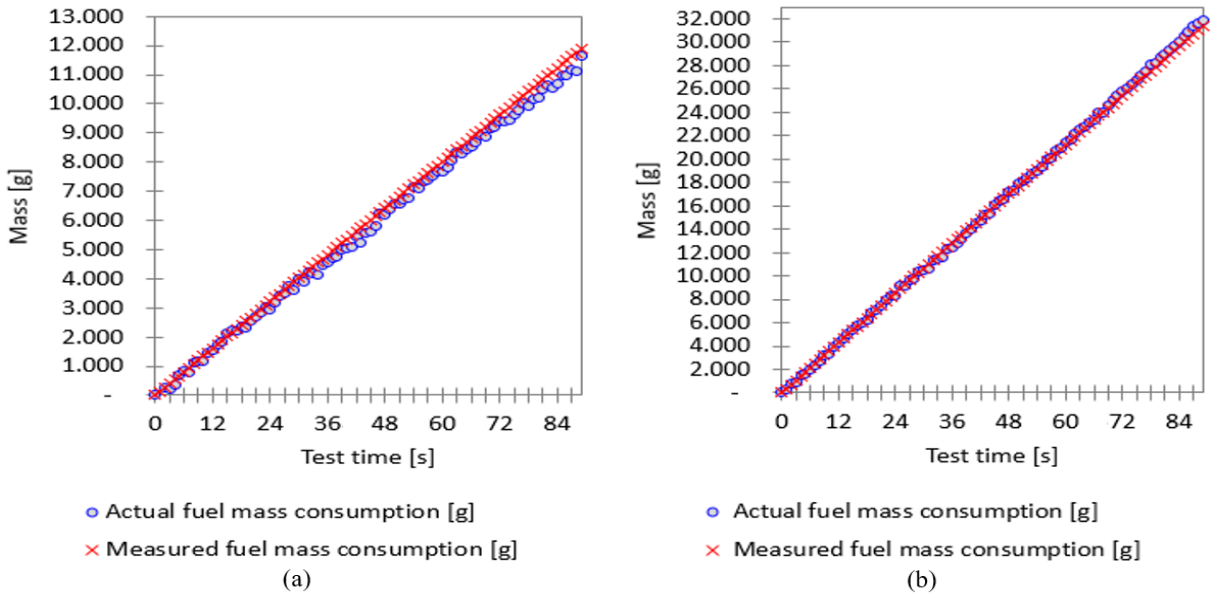

Figure 6 – (a) and (b) shows ethanol mass consumption tests with 1000rpm and inlet pressures equal to 400 and 921mbar, respectively. All graphs were generated using a single and optimized calibration value.

In fig. 6 the graph circles indicate the masses of fuel recorded by the gravimetric balance, and the plus signs indicate the masses recorded by the prototype. The records captured by the gravimetric scale were taken as reference values, so the values recorded by the prototype will be compared to them. These graphs show that the measurements made by the prototype have more linear values during the tests and that the values coming from the gravimetric scale show that there is a linear trend, but they show an irregular deviation point to point. This is because the prototype measurements were made based only on the electronic pulses, which are uniform. Measurements of the gravimetric balance are mainly prone to shocks caused by the motor's functioning and by other external physical factors, such as its uncertainty of measurement, small fluctuations of pressure internal to the Rail, non-repeatability of injection by the electric injector, among others.

For each test scenario, the total mass of fuel consumed, given in grams, as indicated by the gravimetric balance was divided by the total injection time, given in seconds, captured by the prototype during the test. The result of this division represents the best value of the calibration of the prototype for this particular scenario. This verification process is foreseen in the literature when working with physical systems outside the dimensional patterns already studied and tabulated, according (Figliola, Richard S., 2011).

Table 2 shows all test scenarios and their respective calculated calibration parameters.

Table 2 - Test scenarios and their respective calibration parameters in grams per seconds.

		Pure Ethanol (E100). ρ = 805.33 kg/m^3				Gasoline+Ethanol (E27). ρ = 738.5 kg/m^3			
Engine speed (rpm):		1000	2000	3000	4000	1000	2000	3000	4000
Inlet pressures	921mbar:	12.829	12.867	12.925	12.197	11.458	12.002	11.894	12.273
	800mbar:	12.861	12.758	12.665	12.904	11.626	11.933	11.661	12.140
	600mbar:	12.639	12.721	12.626	12.828	10.748	11.822	12.107	12.398
	400mbar:	12.402	12.300	12.795	12.990	11.579	11.058	12.110	12.137
Weighted Mean Calibration Value:		**12.788 g/s**				**11.812 g/s**			

The calculation of the parameters of measurement indicated by each specific scenario were then compared to each other and it was observed that they had a very small standard deviation, which indicates that they point to the same constant that physically represents the union of all the physical parameters and fluid flow adjustment coefficients as detailed in the *Mathematical Formulation* of this paper.

Thus, the deviation between each given value measured by the prototype and the value indicated by the gravimetric scale was considered as punctual error of measure, so the total deviation occurred in the test was considered as the error of the prototype for this scenery. Hence, through this value, we can also calculate the total percentage error of each scenario and have a better idea about the accuracy of the methodology.

The Tab. 3 and Fig. 7 (a) and (b), shows by different way the total percent error calculated for all specifics scenarios with Ethanol and Gasoline tests.

Table 3 – show the total error in milligrams and [**total percent error**] of each particular scenarios

		Pure Ethanol (E100) ρ = 805.33 kg/m^3				Blend of Gasoline and Ethanol 27% (E27) ρ = 738.5 kg/m^3			
Engine speed (rpm):		1000	2000	3000	4000	1000	2000	3000	4000
Inlet pressures	921mbar:	-438.53 [**-1.38%**]	-1129.00 [**-1.74%**]	-2275.22 [**-2.16%**]	-4602.85 [**-3.29%**]	458.55 [**1.99%**]	-1263.85 [**-2.63%**]	-1412.41 [**-1.79%**]	-5243.01 [**-4.81%**]
	800mbar:	-388.86 [**-1.50%**]	-488.44 [**-0.90%**]	-137.05 [**-0.16%**]	-2468.92 [**-1.99%**]	94.46 [**0.49%**]	-839.29 [**-2.07%**]	107.62 [**0.16%**]	-3530.08 [**-3.81%**]
	600mbar:	19.08 [**0.10%**]	-242.62 [**-0.62%**]	97.62 [**0.15%**]	-1318.99 [**-1.45%**]	1138.62 [**8.74%**]	-359.46 [**-1.21%**]	-1651.43 [**-3.52%**]	-4092.89 [**-5.82%**]
	400mbar:	234.70 [**2.01%**]	681.94 [**2.86%**]	-491.87 [**-1.21%**]	-1518.79 [**-2.64%**]	95.33 [**0.90%**]	934.14 [**5.67%**]	-1043.61 [**-3.55%**]	-1645.37 [**-3.73%**]
Mean of total percent error:		**1.51%**				**3.18%**			

From the graphs of Fig. 7 (a) and (b), it can be seen that in both ethanol (E100) and gasoline (E27) the absolute percentage error margin is less than 9% overall error, and for ethanol tests (E100) the percentage error was less than 3.3%.

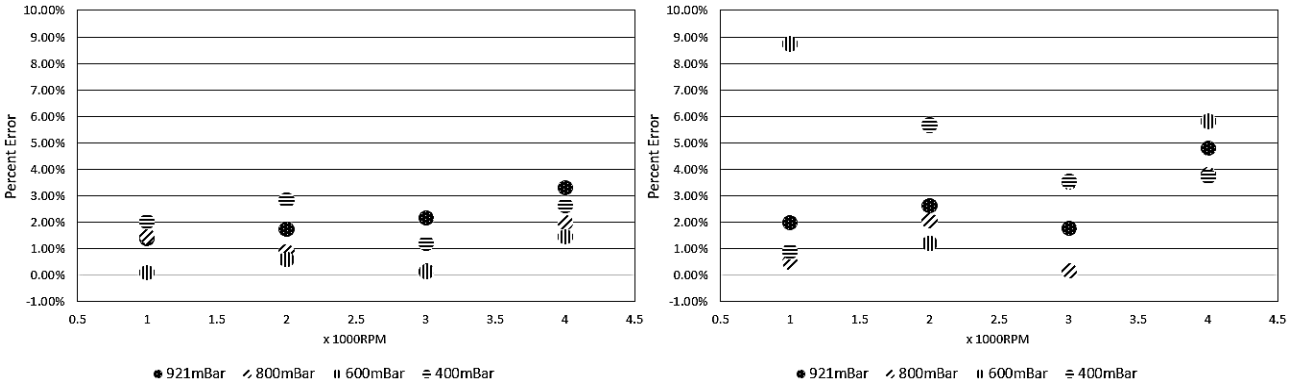

Figure 7 – (a) and (b) shows the total absolute percent error of measured mass of fuel in Ethanol (E100) and Gasoline with 27% Ethanol (E27) respectively.

Finally, when analyzing the real and measured total mass deviation summing all the tests together, the total percentage error was 1.5% for ethanol (E100) and 2.5% for blend (E27).

4. CONCLUSIONS AND FINAL COMMENTS

The results demonstrated that the methodology was more accurate when compared to the 10% accuracy of a typical electromechanical invasive sensor (Furletec, 2013), probably due to the physical and constructive limitations of the same, in counterpart with the fully electronic methodology presented in this paper.

In view of the final results achieved, it can be seen that the simplifying hypotheses considered for the resolution and implementation of the methodology ensured that the total range of the measurement error remained at a satisfactory and viable value, with the advantage that the proposed methodology does not violate the integrity of the original injection circuit of the manufacturers.

Considering that all tests were performed in a very short period of time, only 90 seconds each, it is expected that, in real situations of vehicle use, the percentage error will still be lower than those recorded in this research, with informations provided by (AVL LIST GmbH, 1997), the percentage error presented in measurements of low mass value has greater uncertainties, and that it is better to use this instrument in larger quantities of fuel consumption.

Other advantages provided by the methodology are: the possibility of being installed and implemented in any range of operating pressure and mass flow range of fuel. These features provide a special attraction to the proposed methodology, as they make it adaptable to a large number of different injection systems.

The proposed methodology met the expectation of its idealization, since it provides simple installation and calibration, low cost, works with physical parameters well controlled in the current electronic injection systems, does not require auxiliary sensors like temperature, pressure, uncertainties of the actuators, among others.

5. REFERENCES

Asad, Usman, Raj Kumar, Xiaoye Han, e Ming Zheng. 2011. "Precise instrumentation of a diesel single-cylinder research engine". Measurement 44 (7): 1261–78. https://doi.org/https://doi.org/10.1016/j.measurement.2011.03.028.

AVL LIST GmbH. 1997. "Operating Manual - AVL 733S Dynamic Fuel Meter".

Du, Yiman, Jianping Wu, Senyan Yang, e Liutong Zhou. 2017. "Predicting vehicle fuel consumption patterns using floating vehicle data". Journal of Environmental Sciences 59: 24–29. https://doi.org/10.1016/j.jes.2017.03.008.

Espinosa, Felipe, José A Jiménez, Enrique Santiso, Alfredo Gardel, Diego Pérez, Jesús Casanova, e Carlos Santos. 2011. "Design and implementation of a portable electronic system for vehicle–driver–route activity measurement". Measurement 44 (2): 326–37. https://doi.org/https://doi.org/10.1016/j.measurement.2010.10.006.

Farooqi, Q. R., B. Snyder, and S. Anwar. 2013. "Real time monitoring of diesel engine injector waveforms for accurate fuel metering and control". Journal of Control Science and Engineering. https://doi.org/10.1155/2013/973141.

Ferrari, A., e F. Paolicelli. 2017. "An indirect method for the real-time evaluation of the fuel mass injected in small injections in Common Rail diesel engines". Fuel 191: 322–29. https://doi.org/10.1016/j.fuel.2016.11.053.

Figliola, Richard S., Donald E. Beasley. 2011. Theory and Design for Mechanical Measurements. 5th ed. Danvers: John Wiley & Sons, Inc. http://www.hljp.edu.cn/attachment/20120831082417983.pdf.

Furletec. 2013. "FLOWFUEL30L0 - Diesel and Gasoline Flow Sensor". 2013. http://www.futurlec.com/FLOWFUEL30L0.shtml.

Hakimelahi, Ali, K.V. Krishna Rao, S.L. Dhingra, e Sina Borzooei. 2016. "Fuel Consumption Monitoring for Travel Demand Modeling". Transportation Research Procedia 17 (December 2014): 703–12. https://doi.org/10.1016/j.trpro.2016.11.127.

Herdzik, Jerzy. 2016. "Determination of common rail injector flow characteristics with the use of diesel and biodiesel fuels". Journal of KONES 23 (3): 1–6. https://doi.org/10.5604/12314005.1.

Heywood, John B. 2018. Internal Combustion Engine Fundamentals. Organizado por McGraw-Hill Inc.

Keysight Technologies. 2019. "1146B 100 kHz/100 A Current Probe". 2019. https://www.keysight.com/pt/pd-2329609-pn-1146B/100-khz-100-a-4-current-probe?nid=-32553.1066112&cc=BR&lc=por.

Marcic, Milan. 1999. "A new method for measuring fuel-injection rate". Flow Measurement and Instrumentation 10 (3): 159–65. https://doi.org/10.1016/S0955-5986(98)00053-3.

Orfila, O., C. Freitas Salgeiredo, G. Saint Pierre, H. Sun, Y. Li, D. Gruyer, e S. Glaser. 2017. "Fast computing and approximate fuel consumption modeling for Internal Combustion Engine passenger cars". Transportation Research 50: 14–25. https://doi.org/10.1016/j.trd.2016.10.016.

Pham, P. X., D. Q. Vo, e R. N. Jazar. 2017. "Development of fuel metering techniques for spark ignition engines". Fuel 206: 701–15. https://doi.org/10.1016/j.fuel.2017.06.043.

Sindi Petróleo. 2015. "Testes de Qualidade - Tabelas de Conversões de Produtos".

Szpica, Dariusz. 2018. "Investigating fuel dosage non-repeatability of low-pressure gas-phase injectors". Flow Measurement and Instrumentation 59 (August 2017): 147–56. https://doi.org/10.1016/j.flowmeasinst.2017.12.009.

Tecnology Inc., Microchip. [s.d.]. "PIC18FXX2 Data Sheet - High-Performance, Enhanced Flash, Microcontrollers with 10-Bit A/D". Acessado 16 de fevereiro de 2019. https://ww1.microchip.com/downloads/en/DeviceDoc/39564c.pdf.

Wang, Jinghui, e Hesham A. Rakha. 2016. "Fuel consumption model for conventional diesel buses". Applied Energy 170: 394–402. https://doi.org/10.1016/j.apenergy.2016.02.124.

6. RESPONSIBILITY NOTICE

The authors are the only responsible for the printed material included in this paper.